Supporting Information

Discovery of Fluidic $LiBH_4$ on Scaffold Surfaces and its Application for Fast Co-Confinement of $LiBH_4$-$Ca(BH_4)_2$ into Mesopores

Hyun-Sook Lee,[†] *Son-Jong Hwang,**[‡] *Magnus To,*[‡] *Young-Su Lee, **[†] *and Young Whan Cho*[†]

[†]High Temperature Energy Materials Research Center, Korea Institute of Science and Technology, Seoul 136-791, Republic of Korea

[‡]Division of Chemistry and Chemical Engineering, California Institute of Technology, Pasadena, California 91125, United States

***Corresponding authors:** Son-Jong Hwang E-mail: sonjong@cheme.caltech.edu Tel: +1-626-395-2323; Young-Su Lee E-mail: lee0su@kist.re.kr Tel: +82-2-958-5412.

Supporting Information: The structural characterization of the synthesized SBA-15 was performed. The inset of Figure S1(a) presents Type IV adsorption/desorption isotherm meaning mesoporous products with channel-type pores. The pore size distribution analyzed by Barrett-Joyner-Halenda (BJH) method shown in the inset of Figure S1(a) indicates that the SBA-15 has a pore diameter of ~6.4 nm. Small angle X-ray diffraction (XRD) patterns in Figure S1(b) show clearly the (100), (110), and (200) reflections associated with the two-dimensional hexagonal symmetry (*p6mm*) of SBA-15. The results of N_2 physisorption and small angle XRD depict the successful synthesis of well-ordered periodic mesopore structured SBA-15. The structural parameters are summarized in Table S1.

Table S1. Structural properties of SBA-15.

D_{BJH} (nm)[a]	d_{100} (nm)[b]	a_0 (nm)[c]	W (nm)[d]	S_{BET} (m^2g^{-1})	V_{meso} (cm^3g^{-1})	V_{micro} (cm^3g^{-1})	V_{total} (cm^3g^{-1})
6.3	9.70	11.20	4.90	677.0	0.61	0.16	0.73

[a]D_{BJH} is the maximum value of the BJH pore size distribution peak deduced from the adsorption branch of the N_2 isotherm. [b]d_{100} is the XRD (100) interplanar spacing. [c]a_0 is the unit cell parameter ($a_0 = 2 \times (d_{100}/\sqrt{3})$). [d]W is the pore wall thickness ($W=a_0-D_{BJH}$).

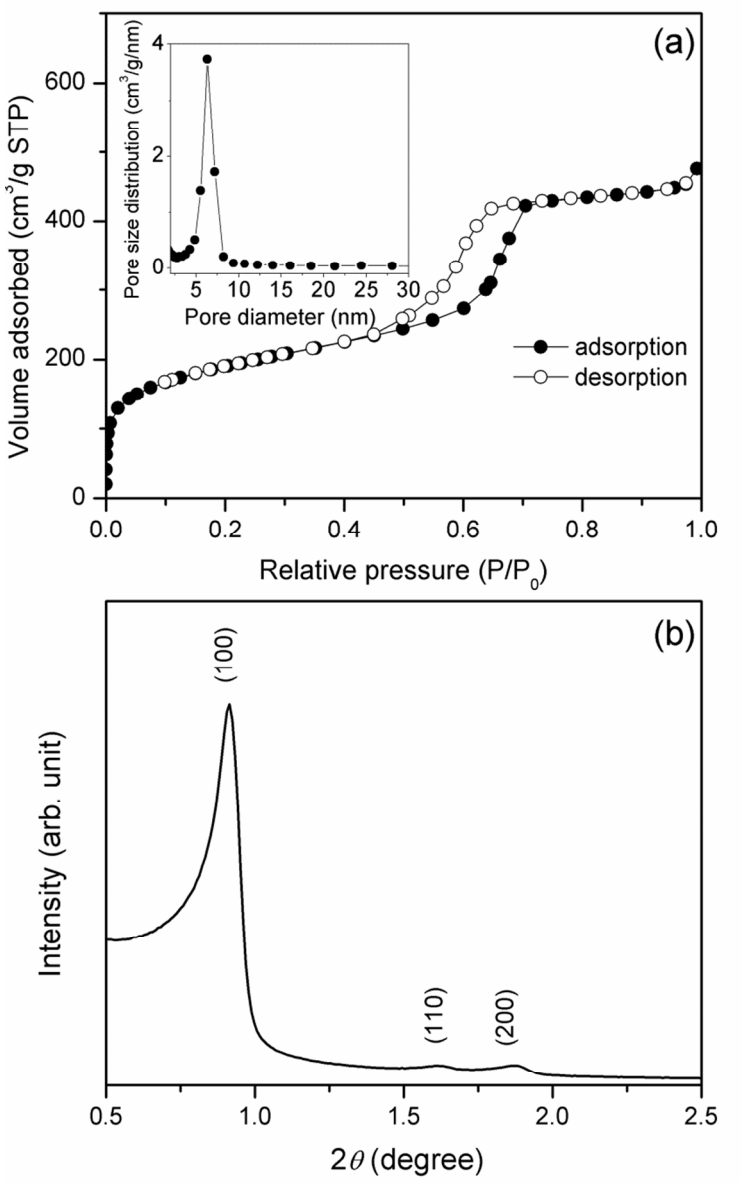

Figure S1. (a) N_2 adsorption and desorption isotherms (inset: Pore size distribution) and (b) X-ray diffraction patterns at small angles for the SBA-15 with 6.3 nm of pore size.

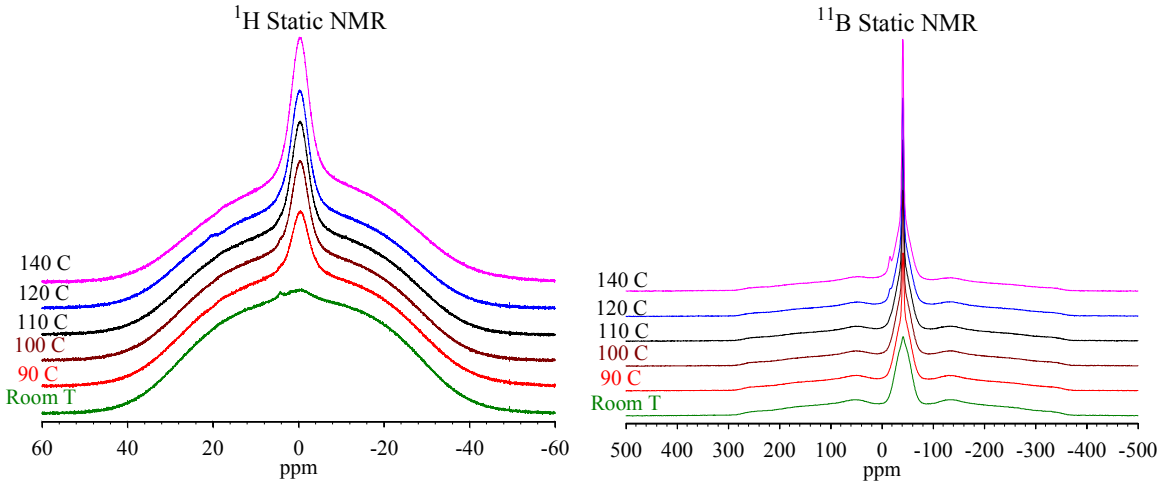

Figure S2. ^{1}H and ^{11}B static NMR spectra of HM-LB/MCM-41 sample recorded at room temperature after heating for 5 hours in a furnace at temperatures listed in spectra. The quadrupole echo sequence was used to recover ^{11}B NMR powder pattern.

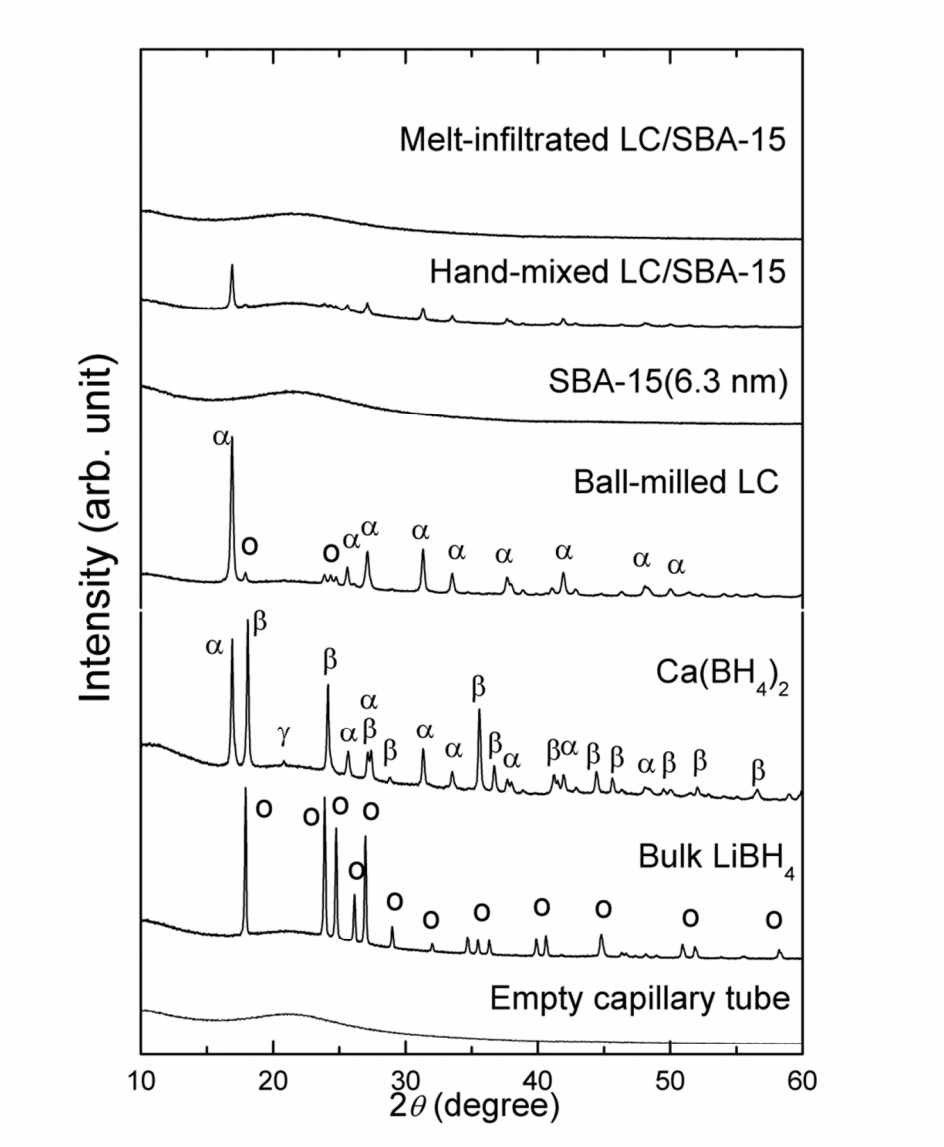

Figure S3. XRD patterns of $LiBH_4$ and $Ca(BH_4)_2$ in bulk phases, ball milled LC, SBA-15, HM-LC/SBA-15, MI-LC/SBA-15 samples (see Table S1 and text). LC ≡ $0.68LiBH_4 + 0.32Ca(BH_4)_2$, an eutectic composition.

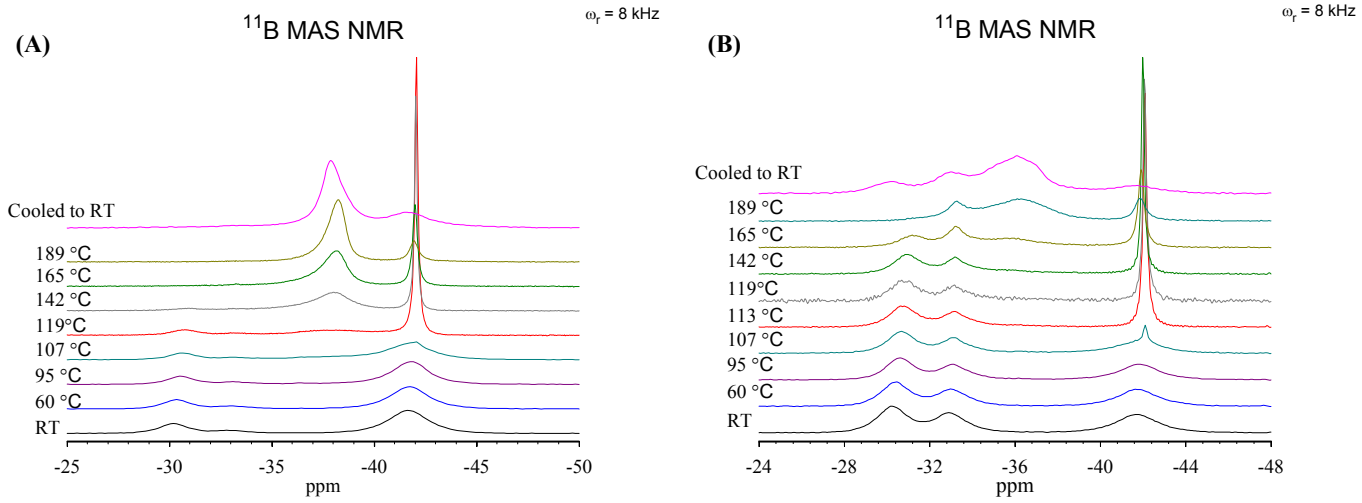

Figure S4. ^{11}B stack plots from *in situ* VT NMR experiments on HM-LC/MCM-41 for non-eutectic compositions of LC ($xLiBH_4$ -$yCa(BH_4)_2$) mixtures. (A) x:y=4:1 mole ratio with $LiBH_4$ being dominant in mixed bulk powder, (B) x:y=1:1.

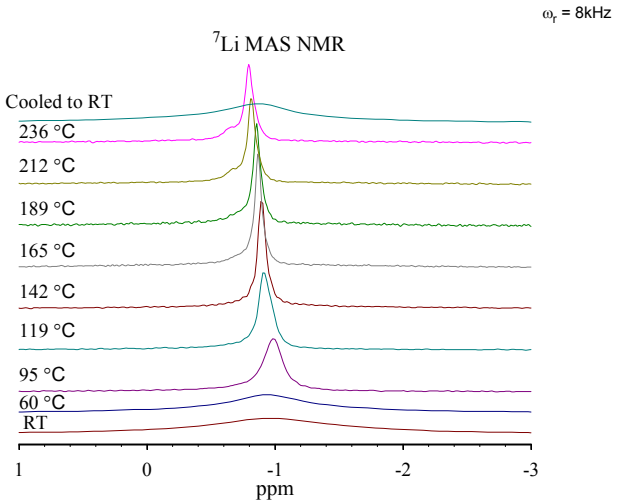

Figure S5. ^{7}Li MAS NMR spectra at various temperatures of the MI-LC/SBA-15 sample.

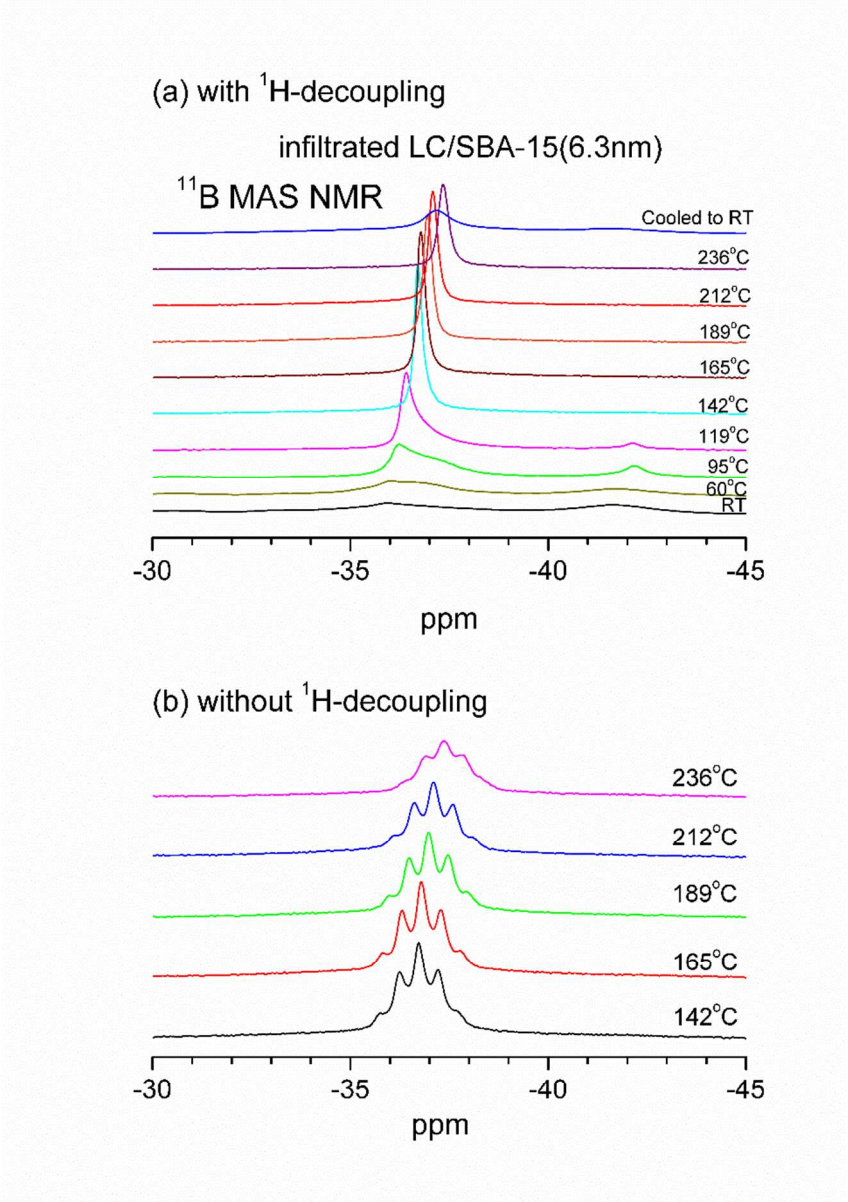

Figure S6. *In situ* ^{11}B VT MAS NMR spectra of the MI-LC/SBA-15 sample, which was measured (a) with and (b) without ^{1}H-decoupling. The melt-infiltration of the sample was performed by heating at 230 °C for 30 min under $p(H_2)$ = 100 bar. Clear splitting patterns of ^{11}B−^{1}H *J*-coupling are observed for the nanoconfined mixed-phase at the temperature above ~120 °C when proton decoupling is applied.

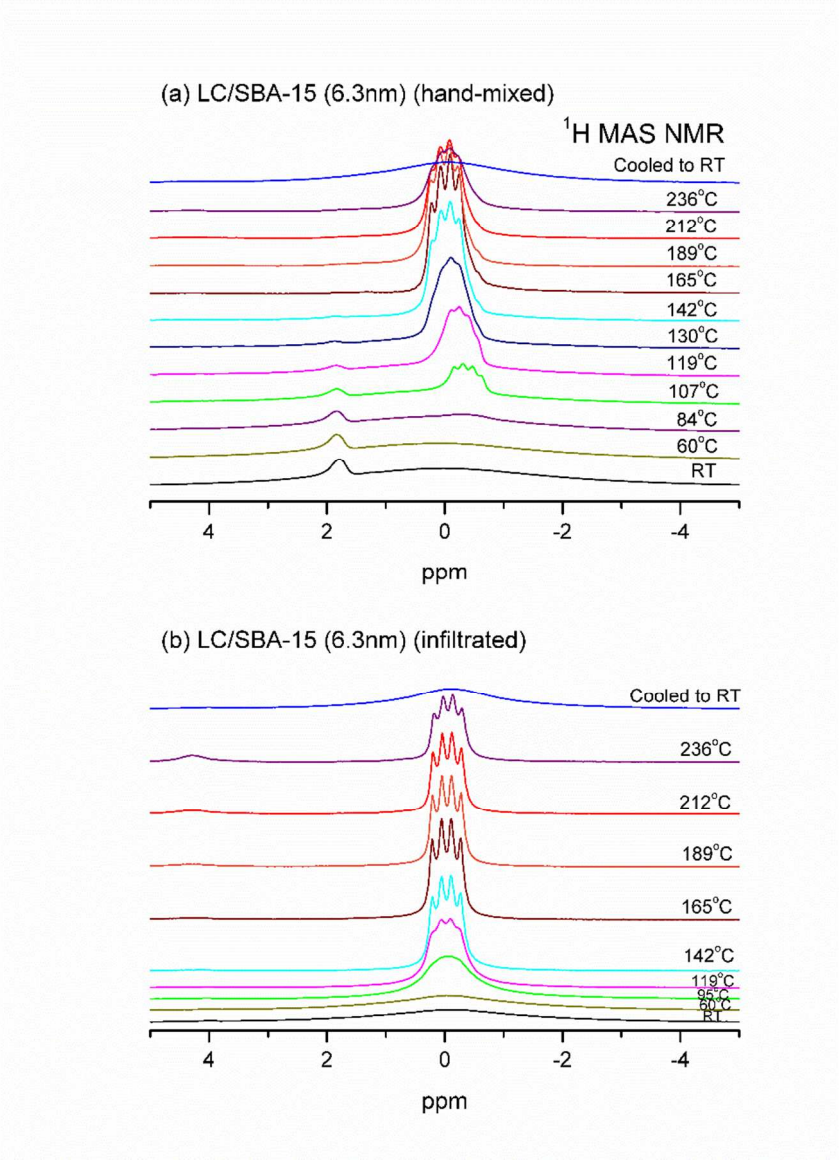

Figure S7. *In situ* ^{1}H VT MAS NMR spectra of (a) HM-LC/SBA-15 and (b) MI-LC/SBA-15 samples.